Cation- and Solvent-Induced Formation of Supramolecular Structures Composed of Crown-Ether Substituted Double-Decker Phthalocyanine Radicals

Naoto Ishikawa* and Youkoh Kaizu

Department of Chemistry, Tokyo Institute of Technology, O-okayama, Meguro-ku, Tokyo, 152-8551, Japan

Received: June 12, 2000; In Final Form: August 17, 2000

Geometric structures of three types of supramolecular aggregates composed of bis(phthalocyaninato)lutetium ($Lu(Pc)_2$) radicals are investigated by means of ESR measurements and theoretical calculations. The tetra-crown-substituted complex, $Lu(CR_4Pc)(Pc)$ (CR_4Pc = tetra-15-crown-5 substituted Pc), forms an aggregate showing an ESR signal of electronic triplet state on addition of cations such as K^+ and NH_4^+, which have a radius large enough to form a 2:1 sandwich-type complex with 15-crown-5. Addition of Na^+ cation, which forms a 1:1 complex with 15-crown-5, did not give rise to such ESR signal. By comparison of the observed zero-field-splitting (zfs) constant D and theoretical calculation on the spin−spin interaction, the assumption that the aggregate has D_{4h} symmetry is confirmed to be reasonable. The center-to-center distance between the two $Lu(Pc)_2$ sites is estimated at 7.0 Å. When no cation is added, $Lu(CR_4Pc)(Pc)$ gives another type of aggregate in methanol/chloroform mixed solvent. This also gives a triplet-state ESR signal with a zfs constant D which is 0.71 times that of the cation-induced ESR. From the theoretical calculation, we concluded that two $Lu(Pc)_2$ sites are placed parallel with a horizontal displacement in the Pc plane. The amount of the displacement is estimated at about 5 Å. The mono-crown substituted complex, $Lu(CR_1Pc)(Pc)$ (CR_1Pc = mono-15-crown-5 substituted Pc), forms a structure linked with one bridge on addition of K^+. The bridge acts as a pivot around which two radical sites can rotate. The zfs constant D obtained from the triplet ESR spectrum is 0.66 times that of the cation-induced system of $Lu(CR_4Pc)(Pc)$. The rotation angle is estimated at about 30−40°. It is suggested, by the calculation of the exchange coupling in the three cases, that spin multiplicity of the ground state can be switched between triplet and singlet depending on the amount of slide or rotation of the $Lu(Pc)_2$ units in the *xy* plane, in which the Pc planes lie.

Introduction

Manipulation of intermolecular forces is a central issue in supramolecular chemistry. To design supramolecular structures, there are a number of choices in forces employed, including metal−ligand coordination bonds and noncovalent bonds based on cation−anion interaction, electric dipole−dipole interaction and hydrogen bonding. As well as understanding of these individual forces, the methodology for control of different forces existing at the same time is also important to construct desired structures.

Bis(phthalocyaninato)lanthanide(III) complexes are known to exist as a stable radical[1] holding an unpaired electron on the HOMO π orbital delocalized over two Pc rings.[2] In solid phase, the complexes exhibit a unique intrinsic conductivity due to the unpaired electron.[3−5] As a static behavior of the π holes, either ferromagnetic or antiferromagnetic behavior is observed in single crystal of $Y(Pc)_2$, depending on the stacking pattern that is determined by the presence or absence of solvent of crystallization.[6] Because of these interesting properties, the bis-(phthalocyaninato)lanthanide complexes are expected to be functional building blocks for supramolecular structures functioning as molecular conducting wire or molecule-based magnet.

To investigate new types of structure composed of bis-(phthalocyaninato)lanthanide, we have synthesized mono-15-crown-5-substituted $Lu(Pc)_2$ complexes, $Lu(CR_1Pc)(Pc)$,[7] and tetra-15-crown-5-substituted $Lu(Pc)_2$ complex, $Lu(CR_4Pc)(Pc)$[8] (Figure 1). In these compounds, two $Lu(Pc)_2$ sites are bound by the 2:1 complex formation of 15-crown-5 and potassium cation. The method employed here is the one first reported by Kobayashi and Lever for the dimer formation of monomeric Pc metal complexes ($M(CR_4Pc)$, M = H_2, Zn, Co, Ni and Cu).[9] We have shown in preliminary reports[7,8] that the substituted $Lu(Pc)_2$ complexes give supramolecular aggregates upon addition of potassium cation in solution. Each system contains two $Lu(Pc)_2$ sites and has two unpaired electrons on the sites separately, composing a biradical.

The purpose of this paper is to investigate geometry of the aggregates composed of $Lu(Pc)_2$ units, as well as the nature of the intermolecular interactions within. We will show that there are three types of structures categorized by the number of bridging sites, which determines the freedom of motion of the systems. The first one is formed with four bridges and has D_{4h} symmetry. The second one is formed with a suitable choice of solvent and has no fixed bridge to hold a rigid geometry. The third type has only one bridging site that acts as a pivot joint, around which the two $Lu(Pc)_2$ sites can rotate. All these three systems are in biradical state and show characteristic ESR spectra with different magnetic parameters. By theoretical calculation on the magnetic parameters that can be compared to those obtained from analysis of the observed ESR spectra, the geometric structures of the aggregates will be discussed. The exchange coupling between the radical sites in the three systems will also be investigated.

10.1021/jp002109z CCC: $19.00
Published on Web 10/07/2000

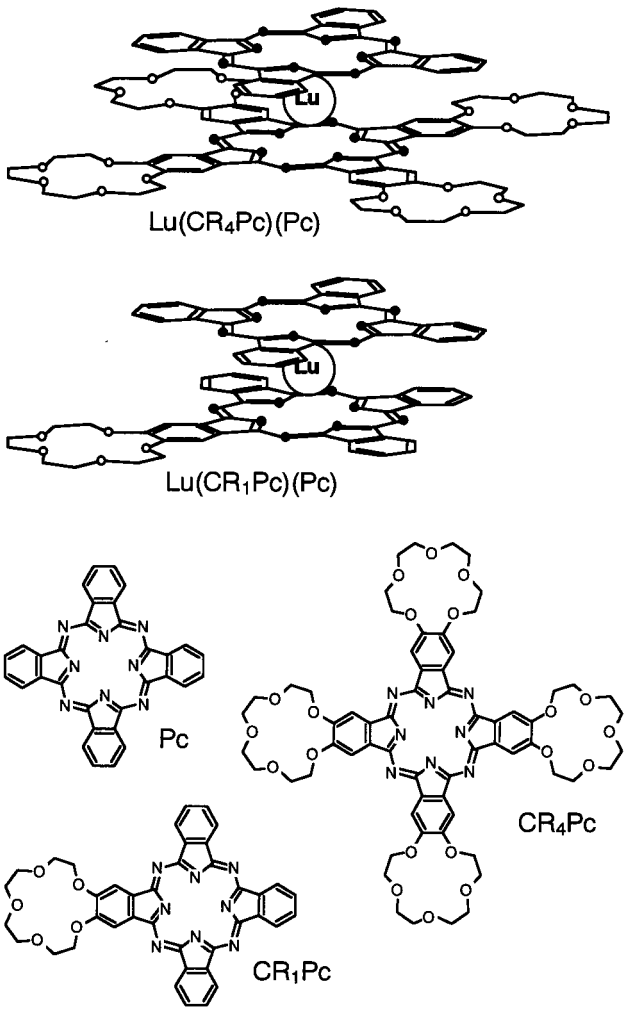

Figure 1. Molecular structure of Lu(CR_4Pc)(Pc) and Lu(CR_1Pc)(Pc).

Experimental Section

Synthesis of Lu(CR_4Pc)(Pc). The metal-free benzo-15-crown-5 substituted phthalocyanine[9] (H_2CR_4Pc, 0.2 g) and the equimolar amount of (phthalocyaninato)lutetium acetate[10] (Lu(Pc)(CH_3COO)(H_2O)$_2$, 0.123 g) were put into dried 1-chloronaphthalene (10 mL). The mixture was refluxed for 8 h, cooled to the room temperature, and added to 50 mL of hexane. The precipitate was extracted with chloroform, and chromatographed on an alumina column (Merck Aluminum oxide 90, particle size 0.063−0.200 mm) with chloroform as eluent. The initial green band was identified as Lu(Pc)$_2$ by UV absorption spectrum. Following the second blue band, Lu(CR_4Pc)(Pc) was obtained as a green band. The green fraction was successively chromatographed twice. Concentration and addition of hexane gave microcrystalline powder of Lu(CR_4Pc)(Pc). The compound was identified by elemental analysis and mass spectroscopy (FAB method on LOEL JMS-HX110/HX110 utilizing MS1 only).

Anal. Calcd for $C_{96}H_{88}O_{20}N_{16}LuCHCl_3$: C, 56.01; H, 4.31; N, 10.77. Found: C, 55.79; H, 4.72; N, 10.13. MS: *m*/*e* 1960.4 (mol wt 1960.4 for $C_{96}H_{88}O_{20}N_{16}Lu$).

Synthesis of Lu(CR_1Pc)(Pc). Dicyanobenzo-15-crown-5 (1 g), dicyanobenzene (2.81 g), lutetium acetate (1.33 g) and 1,8-diazabicyclo[5.4.0]-7-undecene (3.82 g) were put in 100 mL of hexanol, and the mixture was refluxed for 6 h. The mixture was concentrated, added to hexane, and filtered. The precipitate was extracted by dichloromethane and added to hexane to give a viscous mass, which contains non-, mono-, and poly-crown-substituted bis(phthalocyaninato)lutetium and monomeric (phthalocyaninato)lutetium complexes. Succeeding reprecipitations by chloroform/hexane yielded 3.3 g of powdered crude product, which was then subjected to column chromatography to isolate Lu(CR_1Pc)(Pc). First a chloroform solution of the crude product (typically 700 mg in 35 mL of the solvent) was developed with chloroform on an alumina column (Merck Aluminum oxide 90). The first band, which contained radical forms of non-, mono-, and multicrown-substituted bis(phthalocyaninato)lutetium, was collected, concentrated and added to hexane to give a precipitate (about 120 mg from 700 mg of the crude product). Following a filtration, the precipitate was dissolved (typically 30 mg in 25 mL of the solvent) in chloroform/hexane (95/5, v/v) and put on a silica gel column (Merck Silica gel 60, particle size 0.040−0.063 mm). Using chloroform/hexane = 95/5, nonsubstituted complex was first eluted. The second band, which contained only Lu(CR_1Pc)(Pc), was eluted with a sufficient separation from the first and third bands. From this procedure, about 8 mg of Lu(CR_1Pc)(Pc) was isolated. The overall yield of Lu(CR_1Pc)(Pc) was 3%. The compound was identified by elemental analysis and mass spectroscopy (FAB method on JEOL JMS AX-505HA). It was confirmed by the mass spectrum that the sample did not contain non- and poly-15-crown-5-substituted species.

Anal. Calcd for $C_{72}H_{46}N_{16}O_5Lu\cdot CHCl_3$: C, 58.08; H, 3.14; N, 14.85. Found: C, 58.05; H, 3.33; N, 14.79. MS: *m*/*e* 1389.3 (mol wt 1389.3 for $C_{72}H_{46}N_{16}O_5Lu$).

Measurement. Absorption spectra were measured on a Hitachi spectrophotometer 330. ESR spectra were obtained with a JEOL-RE1X spectrometer operating at X-band frequency. The solvents used for the spectral measurements were purified by distillation.

Calculational Methods

π-Electron Systems of Lu(Pc)$_2$. Zero field splitting constants and the exchange coupling were calculated using MOs of Lu(Pc)$_2$, which were obtained by a semiempirical quantum chemical method within the π approximation described previously.[11−14] The open shell Lu(Pc)$_2$ was dealt with by the restricted open-shell Hartree−Fock (ROHF) method,[15] in which a single set of spatial functions is used for both α and β spin orbitals. Parameters[16−18] and formulas to evaluate molecular integrals used for the calculation were the same as those used previously for Pc monomer,[11] dimer,[12,13] and trimer.[14,19] The geometry of Lu(Pc)$_2$ was approximated as a set of two Pc macrocycles being placed in parallel with a common C_4 axis. The interplanar distance was set at 3.0 Å. The torsion angle between the Pc rings around the C_4 axis was assumed to be 45°. The Lu ion was treated as a +3 point charge.

Zero Field Splitting (zfs) Constants of a Triplet State. The electronic spin−spin interaction between the two unpaired electrons in orbitals ϕ_A on the site A and ϕ_B on the site B, A and B being the component Lu(Pc)$_2$ radicals, is written as a tensor $\mathbf{D}$[20]

$$\mathbf{D} = -\frac{3}{4}\frac{\mu_0}{4\pi}g^2\beta^2\{\langle\phi_A(1)\,\phi_B(2)\,|\hat{\mathbf{D}}|\phi_A(1)\,\phi_B(2)\rangle - \langle\phi_A(1)\,\phi_B(2)\,|\hat{\mathbf{D}}|\phi_A(2)\,\phi_B(1)\rangle\} \quad (1)$$

where

$$\hat{\mathbf{D}} = \begin{pmatrix} \frac{r_{12}^2 - 3x_{12}^2}{r_{12}^5} & \frac{-3x_{12}y_{12}}{r_{12}^5} & \frac{-3x_{12}z_{12}}{r_{12}^5} \\ \frac{-3x_{12}y_{12}}{r_{12}^5} & \frac{r_{12}^2 - 3y_{12}^2}{r_{12}^5} & \frac{-3y_{12}z_{12}}{r_{12}^5} \\ \frac{-3x_{12}z_{12}}{r_{12}^5} & \frac{-3y_{12}z_{12}}{r_{12}^5} & \frac{r_{12}^2 - 3z_{12}^2}{r_{12}^5} \end{pmatrix}$$

For the orbitals ϕ_A and ϕ_B, we chose the singly occupied orbital of $Lu(Pc)_2$, which belong to a_2 representation in D_{4d} point group.[12,13] The orbitals are the one obtained by a calculation for an isolated $Lu(Pc)_2$ radical. The second term of eq 1 is negligible because we are dealing with orbitals belonging to different sites. The first term in eq 1 is expanded in AO basis $\{\chi_{iA}\}$ and $\{\chi_{jB}\}$ using LCAO MO coefficients C_{iA} and C_{jB}, and approximated as follows

$$\langle \phi_A(1)\,\phi_B(2)\,|\hat{\mathbf{D}}|\phi_A(1)\,\phi_B(2)\rangle = \sum_{ijkl} C_{iA}C_{jA}C_{kB}C_{lB}(\chi_{iA}\chi_{jA}|\hat{\mathbf{D}}|\chi_{kB}\chi_{lB}) \approx \sum_{ij} C_{iA}^2 C_{jB}^2 (\chi_{iA}\chi_{lA}|\hat{\mathbf{D}}|\chi_{jB}\chi_{jB})$$

Each matrix element of $(\chi_{iA}\chi_{lA}|\hat{\mathbf{D}}|\chi_{jB}\chi_{jB})$ is calculated using point dipole approximation:

$$(\chi_{iA}\chi_{iA}|\hat{D}_{11}|\chi_{jB}\chi_{jB}) \approx \frac{r_{ij}^2 - 3x_{ij}^2}{r_{ij}^5},$$

$$(\chi_{iA}\chi_{iA}|\hat{D}_{12}|\chi_{jB}\chi_{jB}) \approx \frac{-3x_{ij}y_{ij}}{r_{ij}^5}$$

and other terms are calculated likewise. Here, r_{ij} is the distance between the center of χ_{iA} and that of χ_{jB}, and x_{ij}, y_{ij}, z_{ij} are the x, y, z components of the vector $\mathbf{r}_{ij}$, respectively.

Diagonalization of $\mathbf{D}$ gives a diagonal matrix $\mathbf{D}^d$ with matrix elements D_{xx}, D_{yy} and D_{zz}. Assigning the element with the largest absolute value to D_{zz}, two independent parameters, the following definitions for D and E are used.

$$D = \frac{-3D_{zz}}{2} \tag{2}$$

$$E = -\frac{1}{2}(D_{xx} - D_{yy}) \tag{3}$$

Electron Exchange Coupling between the Radicals. The exchange coupling defined by

$$J = -\frac{1}{2}\{(\text{triplet-state energy}) - (\text{singlet-state energy})\} \tag{4}$$

in the biradical systems composed of two $Lu(Pc)_2$ sites were calculated under the standard Heitler-London treatment using the following equation:

$$J = \frac{1}{1-s^4}[(\phi_A\phi_B|\phi_B\phi_A) + s\{(\phi_A|V_A|\phi_B) + (\phi_B|V_B|\phi_A)\} - s^2\{(\phi_A|V_B|\phi_A) + (\phi_B|V_A|\phi_B) + (\phi_A\phi_A|\phi_B\phi_B)\}]$$

Here, s is the overlap integral between the singly occupied orbitals ϕ_A on the site A and ϕ_B on the site B. To calculate the term due to the potential V_A and V_B which the "core" $[Lu(Pc)_2]^+$ makes, the electric charge from the electron population on each AO was replaced with a point charge on the nucleus to which the AO belongs.

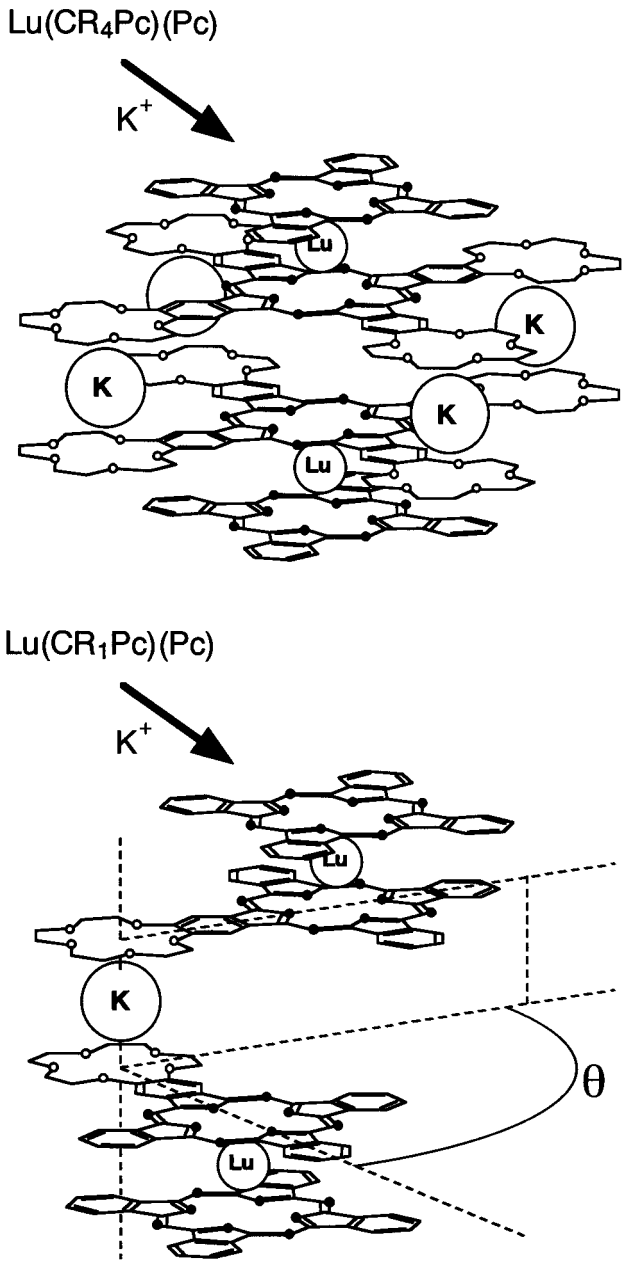

Figure 2. Proposed supramolecular structures composed of $Lu(CR_4Pc)(Pc)$ and $Lu(CR_1Pc)(Pc)$ with the presence of potassium cation.

Results and Discussion

Cation-Induced Aggregation of $Lu(CR_4Pc)(Pc)$. The π-radical $Lu(CR_4Pc)(Pc)$ shows an ESR spectrum at $g = 2.002$ in frozen solution in chloroform at 77 K as shown in Figure 3a. The g value and the spectral shape are similar to those of unsubstituted complex $Lu(Pc)_2$. Addition of CH_3COONa does not give any new signal (Figure 3b). With addition of CH_3COOK, a new signal appears (Figure 3c-1) on both sides of the mono-radical signal. The separation between the main peaks is 4.65 mT. The new signal has a typical shape of ESR signal of electronic triplet state in a random orientation. The triplet signal is an evidence of a formation of an aggregate in a biradical state.

Ammonium ion is also known to form an 1:2 complex with 15-crown-5 as potassium cation. When CH_3COONH_4 is used,

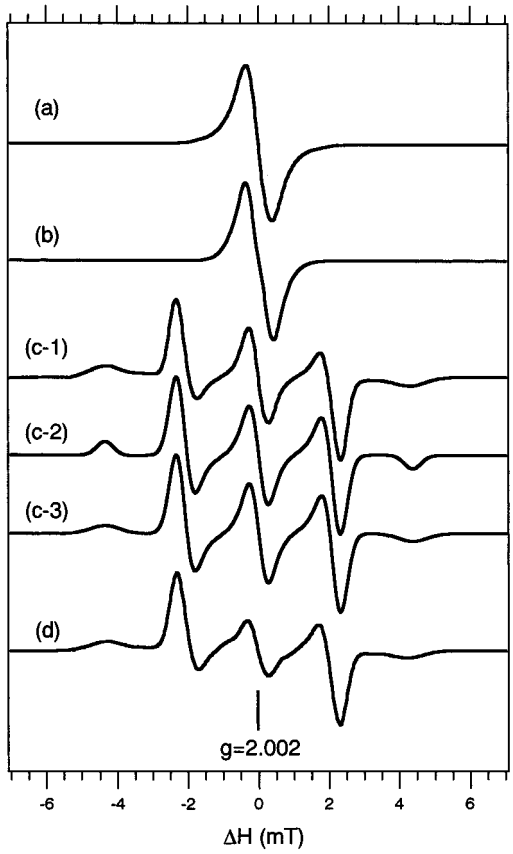

Figure 3. X-band ESR spectra of Lu(CR_4Pc)(Pc) under the presence of (a) no cation, (b) CH_3COONa, (c-1) CH_3COOK, (d) CH_3COONH_4 in frozen solution at 77 K in (a) $CHCl_3$ and (b, c-1 and d) $CHCl_3$:MeOH = 50:50. The concentration of the added salt is 1.2×10^{-1} M in each case except (a), and that of Lu(CR_4Pc)(Pc) is 1×10^{-4} M. The simulations for the case (c-1) are shown in (c-2) and (c-3). The triplet ESR part is obtained with the zero-field splitting $D = 0.00407$ cm^{-1} (4.35 mT), using a Gaussian line shape of isotropic line-width $w =$ 0.28 mT in (c-2) and anisotropic line-width $w_{zz} = 0.48$ mT and $w_{xx} = w_{yy} = 0.28$ mT in (c-3). The doublet ESR part is obtained with isotropic hfs constants from Lu $a_{Lu} = 0.05$ mT, $a_{N(1)} = 0.04$ mT and $a_{N(2)} = 0.04$ mT using Lorentzian line shape with hwhm = 0.31 mT in both (c-2) and (c-3).

a similar signal to the K^+-induced ESR is observed as shown in Figure 3d. The separation between the main peaks is 4.63 mT, which is almost the same as the K^+ case. This indicates that the NH_4^+-indiced system has basically the same geometry as that of K^+-induced one.

Solvent-Induced Aggregation of Lu(CR_4Pc)(Pc). When the potassium ion is absent in the solution, an indication of another type of structure is observed. Figure 4 shows ESR spectra at 77 K with different ratios of chloroform/methanol. With 5% of methanol in the solution, an additional signal appears (Figure 4b). This signal grows as the proportion of methanol increases as shown in Figure 4c. The case where chloroform/methanol = 50/50 clearly shows the signal of a triplet state (Figure 4d). The separation between the main peaks is 3.25 mT. The separation is smaller than that of the cation-induced triplet signals. This indicates that the mean distance between the two unpaired electrons in the present case is larger than that in the cation-induced case. Regardless of the ratio of the chloroform and methanol, addition of CH_3COOK annihilated the methanol-induced signal and gave rise to the K^+-induced signal.

The unsubstituted Lu$(Pc)_2$ did not show any new signal by the addition of methanol. This indicates that the presence of the crown parts is essential for the solvent-induced dimerization.

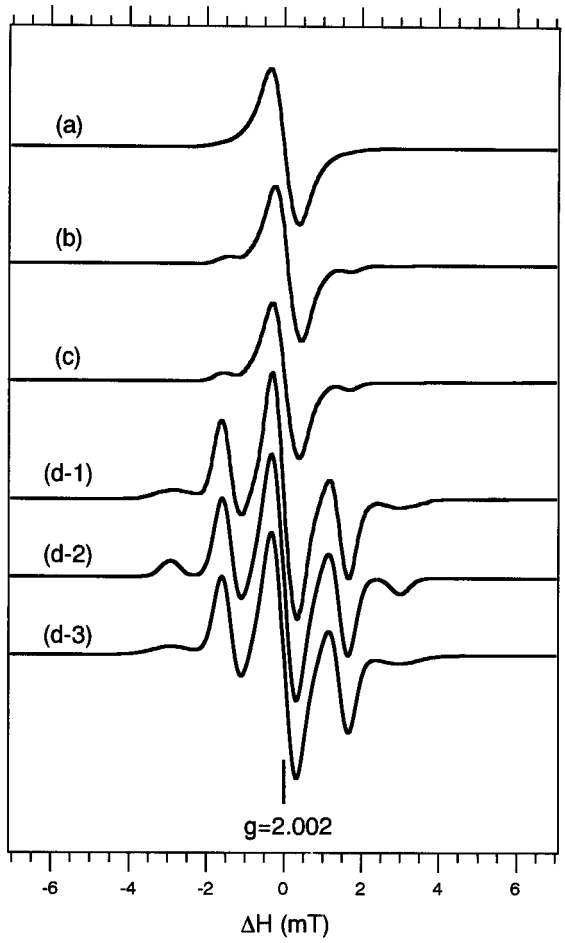

Figure 4. X-band ESR spectra of Lu(CR_4Pc)(Pc) (a) in $CHCl_3$, (b) in $CHCl_3$:MeOH = 95:5, (c) in $CHCl_3$:MeOH = 90:10, (d-1) in $CHCl_3$:MeOH = 50:50. Each spectrum was taken at 77 K in a frozen solution. The concentration of Lu(CR_4Pc)(Pc) is 1×10^{-4} M. The simulations for the case (d-1) are shown in (d-2) and (d-3). The triplet ESR part is obtained with the zero-field splitting $D = 0.00277$ cm^{-1} (2.96 mT), using a Gaussian line shape of isotropic line-width $w = 0.28$ mT in (d-2) and anisotropic line-width $w_{zz} = 0.56$ mT and $w_{xx} = w_{yy} = 0.28$ mT in (d-3). The doublet ESR part is obtained with isotropic hf constants from Lu $a_{Lu} = 0.07$ mT, $a_{N(1)} = 0.04$ mT and $a_{N(2)} = 0.04$ mT using Lorentzian line shape with a hwhm = 0.31 mT in both (d-2) and (d-3).

Separation of Cationic Effect and Solvent Effect in Aggregation of Lu(CR_4Pc)(Pc). Here, we again investigate Figure 3. The 15-crown-5 forms 1:1 complex with Na^+, which has a smaller radius than K^+. As expected, addition of CH_3-COONa did not cause biradical formation (Figure 3b). More important point, however, is the fact that the addition of Na^+ annihilates the methanol-induced signal. This indicates that the crown moieties are occupied by Na^+, and even with high ratio of methanol, methanol-induced biradical formation is inhibited owing to the electrostatic repulsion between the positively charged $[Lu(CR_4Pc)(Pc)Na_n]^{n+}$ ions. Additionally, this experiment suggests that the CH_3COO^- ion does not contribute to the formation of the aggregates.

Cation-Induced Aggregation of Lu(CR_1Pc)(Pc). Figure 5 shows a set of ESR measurements for the mono-crown Pc dimer. The signal in chloroform solution shown in Figure 5a is similar to the Lu$(Pc)_2$ and Lu(CR_4Pc)(Pc). The measurement in a mixed solvent with chloroform and methanol at the ratio of 50/50 shows an additional signal on both sides of the original signal (Figure 5b). However, the intensity of the new signal is much

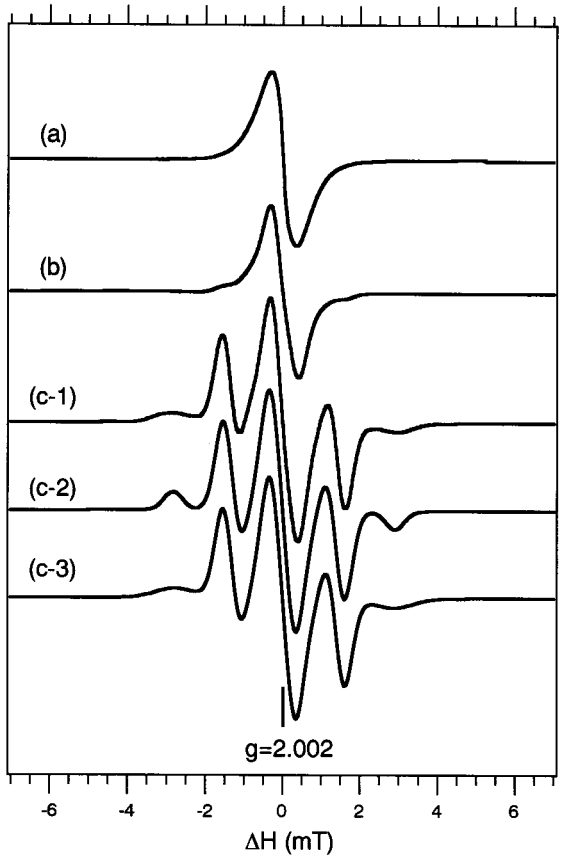

Figure 5. X-band ESR spectra of Lu(CR_1Pc)(Pc) (a) in $CHCl_3$, (b) in $CHCl_3$:MeOH = 1:1, (c-1) with CH_3COOK (1.2×10^{-1} M) in $CHCl_3$:MeOH = 1:1. The concentration of Lu(CR_1Pc)(Pc) is 1×10^{-4} M. Each spectrum was taken at 77 K in a frozen solution. The simulations for (c-1) are shown in (c-2) and (c-3). The triplet ESR part is obtained with the zero-field splitting $D = 0.00268$ cm^{-1} (2.86 mT), using a Gaussian line shape of isotropic line-width $w = 0.28$ mT in (c-2) and anisotropic line-width $w_{zz} = 0.56$ mT and $w_{xx} = w_{yy} = 0.28$ mT in (c-3). The doublet ESR part is obtained with isotropic hf constants from Lu $a_{Lu} = 0.08$ mT, $a_{N(1)} = 0.05$ mT and $a_{N(2)} = 0.04$ mT using Lorentzian line shape with a hwhm = 0.31 mT in both (c-2) and (c-3).

smaller than the case of the tetra-crown Pc dimer shown in Figure 4d-1). This indicates that the solvent-induced dimerization is less efficiently achieved when the number of crown parts is decreased. Addition of CH_3COOK gives a new signal (Figure 5c-1). The separation between the main peaks is 3.12 mT. This value is smaller than that of K^+-induced signal in Lu(CR_4Pc)(Pc) and similar to that of the solvent-induced signal in Lu(CR_4Pc)(Pc).

Simulations of the ESR Spectra. Figure 3c-2 is a simulation for the observed spectrum (c-1). The displayed is the sum of the signal of biradical (at $\Delta H = \pm 2.3$ and ± 4.3 mT) and that of monoradical (at $\Delta H = 0$ mT). The biradical component is obtained assuming a triplet state, with a zfs constant $|D| = 0.00407$ cm^{-1} (4.35 mT) and $g = 2.002$. The line shape employed here is a Gaussian shape with a half-width-at-half-maximum (hwhm) of 0.28 mT, to which all the hyper-fine (hf) structures from Lu and N nuclei are assumed to be incorporated. The signal of the mono-radical in doublet state is simulated with hf constants 0.05 mT for the Lu^{175} ($I = {}^7/_2$), 0.04 mT for the eight N ($I = 1$) atoms of one of the two types, and 0.04 mT for the other eight N atoms, using Lorentzian line shape with hwhm $w = 0.31$ mT. As seen in the figure, the overall agreement is acceptable. However, the width at the signal at $\Delta H = \pm 4.3$ mT, which corresponds to the principal axis *z*, is not well reproduced. Figure 3c-3 is a calculation using the same parameters except for the line width: the hwhm was assumed to be a tensor with principal values of $w_{zz} = 0.48$ mT and $w_{xx} = w_{yy} = 0.28$ mT. The agreement to the experiment is improved in the second calculation. This indicates that there is a large anisotropy in the line width. Since all the hf structures are incorporated in a Gaussian line shape, its hwhm is directly reflected from the value of the hf constants. The anisotropy of the hwhm should be attributed to that of the hf constant of Lu or N nuclei.

The simulation was also carried out for the solvent-induced biradical signal of Lu(CR_4Pc)(Pc). Figure 4d-2 was obtained with the zfs constants $|D| = 0.00277$ cm^{-1} (2.96 mT), $E = 0$ cm^{-1} and isotropic hwhm, $w = 0.28$ mT. As in the cation-induced case, a disagreement with the experimental data is observed at $\Delta H = \pm 2.8$ mT. To fit the simulation, it was needed to treat the hwhm value as a tensor with principal values of $w_{zz} = 0.56$ mT and $w_{xx} = w_{yy} = 0.28$ mT (Figure 4d-3). The smaller zfs constant $|D|$ indicates that the mean distance between the two radical sites is longer than the cation-induced case.

Calculations for cation-induced biradical signal of the mono-crown Pc dimer are shown in Figure 5c-2 and c-3. The former is obtained with isotropic hwhm at $w = 0.28$ mT and zfs constants $|D| = 0.00268$ cm^{-1} (2.86 mT) and $E = 0$ cm^{-1}. The latter is the best reproduction which is obtained using the same zfs constants and a tensor line width with principal values $w_{zz} = 0.56$ mT and $w_{xx} = w_{yy} = 0.28$ mT. This case also shows anisotropy in the line width.

Theoretical Calculation of zfs Constants and Exchange Interaction in the Aggregates. When four potassium cations bind two Lu(CR_4Pc)(Pc) molecules, the resultant structure is in D_{4h} symmetry as shown in Figure 2. The variable that determines the zfs constants and exchange interaction in this case is the distance between the two radical sites along the common C_4 axis. In contrast, the solvent-induced aggregation does not have any bridge that fixes relative geometry rigidly and can have different symmetry. Because of the smaller zfs constant $|D|$, the solvent-induced system is expected to have a larger distance than the cation-induced one. For the same reason, the cation-induced system from Lu(CR_1Pc)(Pc) also seems to have a larger mean-distance which is a result of the rotation around the pivot point at the single bridging cation. In this section, to determine the geometric structure of the aggregates, zfs constants are calculated in a function of a variable that determines the distance between the two radical sites in several different arrangements. In each case, the exchange interaction is investigated to determine the spin multiplicity of the ground state.

(1) Cation-Induced D_{4h} Structure from Lu(CR_4Pc)(Pc). Figure 6a shows calculated zfs constant *D* for the biradical system in a configuration shown in the Scheme 1. Each unpaired electron is separately put on one of the two Lu$(Pc)_2$ sites, which are placed parallel with a center-to-center distance Δz. The zfs constant *D* is predicted to take negative values in the region $\Delta z > 6$ Å. Since the configuration is assumed to have an axial symmetry, another zfs constant *E* is zero. From the plot, the center-to-center distance is estimated at about 7.0 Å, which corresponds to the experimentally obtained zfs constant ($|D| = 0.00407$ cm^{-1}). This value is about 0.5 Å larger than the distance[21] in crystal of unsubstituted lanthanide bis(phthalocyaninato) complexes: they are 6.5 Å in Lu$(Pc)_2 \cdot CH_2Cl_2$,[22,23] 6.47 Å in Y$(Pc)_2 \cdot CH_2Cl_2$,[6] and 6.58 Å in Nd$(Pc)_2$.[24] On the other hand, an X-ray diffraction experiment on columnar discotic mesophase of Lu$(Pc(CH_2OC_{18}H_{37})_8)_2$ have shown that the distance between the Lu atoms in a column is 7.3 Å.[25] The

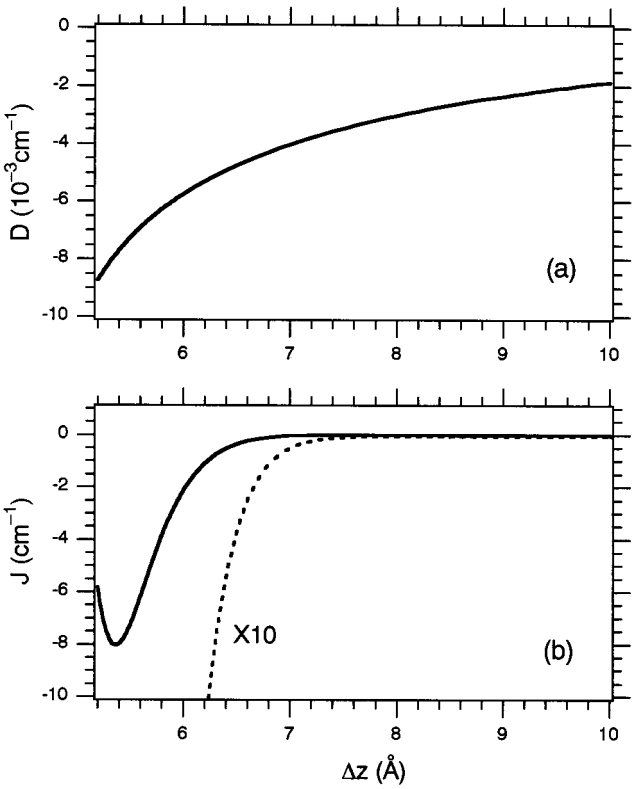

Figure 6. Plots of (a) zero-field splitting constant *D* and (b) exchange interaction *J* in a function of the distance Δz defined in Scheme 1.

SCHEME 1

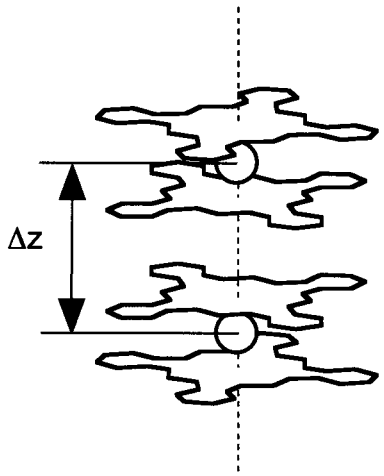

calculated value 7.0 Å in the present case appears reasonable since it is larger than that of unsubstituted complexes and shorter than that of a complex substituted with bulky alkyl chains with no bridging. The calculation clearly shows that the assumed structure shown in Figure 2 is valid.

The most probable factor that increases the intermolecular distance would be the higher steric hindrance: the two CR_4Pc rings in the present case are in completely overlapped positions, while such a overlap between the adjacent Pc rings in the crystals of lanthanide Pc complexes is reduced by rotation or slide.

In isolated 2:1 complexes of 15-crown-5 and the cations, the distance between the center of the five coordinating oxygen atoms of a crown and that of the counterpart crown is reported at 3.33 Å for $(15\text{-crown-5})_2K\cdot I_3\cdot(I_2)_3$,[26] 3.34 Å for (benzo 15-crown-5) $_2K\cdot I$,[27] and 3.65 Å for $(15\text{-crown-5})_2NH_4\cdot UO_2\cdot Cl_4$.[28]

SCHEME 2

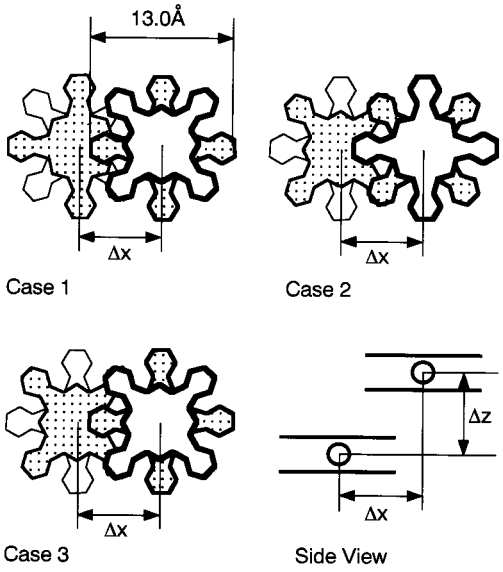

These values are smaller than the distance between the CR_4Pc rings in the cation-induced structure (4.0 Å = 7.0 Å − 3.0 Å). Since the crown parts are flexible to an extent, the longer distance in the present case should be achieved by widening the crown-crown separation at the atoms near the Pc.

The exchange coupling *J*, which is defined by eq 4, takes a negative value in the region larger than 6 Å as seen in Figure 6b. Its absolute value is decreasing as Δz increases along the C_4 axis. The variation of *J* with respect to Δz is much more sensitive than that of *D*. In the present model, *J* is estimated at -0.35 cm^{-1} when Δz = 6.5 Å, and -0.04 cm^{-1} when Δz = 7.0 Å. In the configuration where two Pc dimer radicals are aligned along the C_4 axis, the overall electronic state of the system is predicted to be singlet.

(2) Solvent-Induced Aggregate of Lu(CR_1Pc)(Pc). From the fact that the solvent-induced triplet-state ESR does not occur in $Lu(Pc)_2$, the formation of the radical pair in $Lu(CR_4)(Pc)$ is caused by the presence of the crown parts. If we assume the solvent-induced structure has common C_4 axis as the above D_{4h} case, Δz is estimated at 8.4 Å. This is 1.4 Å longer than that of cation-induced system, indicating that this is not a reasonable assumption.

Another possibility is a configuration where two sites are arranged parallel with a slide to a direction in the Pc planes. Scheme 2 describes this situation. Δz is the amount of the displacement to a direction in the Pc planes. To generalize the discussion, three different configurations are considered as shown in the Scheme 2. Since the crown parts play an essential role in aggregation, we can assume that the CR_4Pc ligands are at the inner positions (shaded in the Scheme 2). In case 1, an axis connecting opposite coordinating nitrogen atoms in a ligand is parallel to either *x* or *y* coordinate in each CR_4Pc ring. In case 2, the angle between an N−N axis and the *x* (or *y*) coordinate is 45° in each CR_4Pc, while in case 3 the axis is 0° or 90° in a CR_4Pc and 45° in the other. The height Δz at which the counterpart $Lu(Pc)_2$ site is placed is set at 7.0 Å, which is the value obtained in the preceding section.

Figure 7a shows the results of the calculations of *E* with varied Δx for the three cases. When $\Delta x \neq 0$, C_4 axis in the radical pair vanishes and *E* can take a nonzero value. The absolute value of *E* becomes maximum at 6−8 Å.

The *D* term takes a negative value and approaches zero with increase of Δx as shown in Figure 7b. From the observed |*D*|/

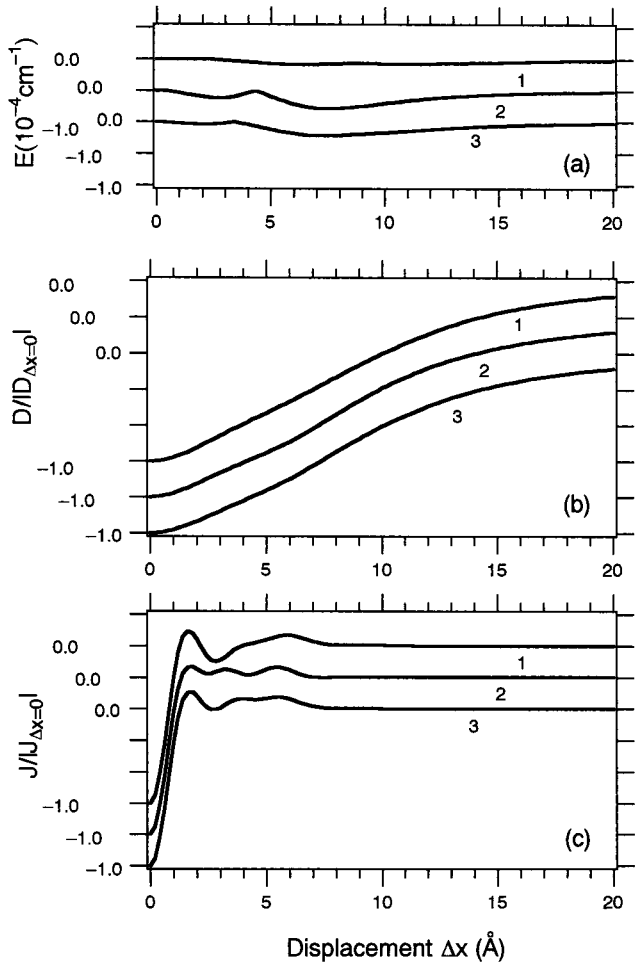

Figure 7. Plots of (a) zero-field splitting constants *E*, (b) *D* and (c) exchange interaction *J* in a function of relative displacement Δ*x* defined for the cases 1, 2, and 3 in Scheme 2. Δ*z* is set at 7.0 Å.

$|D_{\Delta x=0}|$ ratio (0.00288 cm^{-1}/0.00407 cm^{-1} = 0.71), Δ*x* is predicted at 5.4 Å in case 1, 5.7 Å in case 2 and 5.8 Å in case 3. In these cases, the *E* value is negligibly small so that including *E* to the ESR spectrum simulation gave practically no effect on the result in Figure 4.

Interestingly, the calculated Δ*x* values are close to the corresponding values reported in the $Lu(Pc)_2 \cdot CH_2Cl_2$ crystal (4.7 Å) and $Y(Pc)_2 \cdot CH_2Cl_2$ crystal (4.6 Å). This suggests that the amount of slide along the Pc plane is determined solely by the nature of $Lu(Pc)_2$ part, although the crown parts play a role in bring the complexes close. Once two $Lu(Pc)_2$ parts are in a face-to-face position, sliding about 5 Å may stabilize the entire system.

Figure 7c shows calculated *J* in the function of Δ*x*. The value of *J* varies significantly with Δ*x*, making a clear contrast to the *J* vs Δ*z* plot. The most remarkable prediction by the calculation is that as soon as Δ*x* departs from zero, *J* values rapidly turn form negative to positive. Although case 1 has a region where *J* returns to negative value, in most of the region Δ*x* > 1.3 Å, *J* is positive. In those regions the electronic state of the system is triplet.

(3) Cation-Induced Aggregate of Lu(CR$_1$Pc)(Pc). As indicated by the ESR spectrum, two mono-crown Pc dimers are bound by a potassium cation. The resultant structure has only one bridge site, which can act as a pivot, around which the two $Lu(Pc)_2$ sites can rotate. However, as seen in the ESR spectrum, such rotation appears to be restricted so that the zfs constant *D* (and *E*) is uniquely determined. Figure 8 shows calculated of

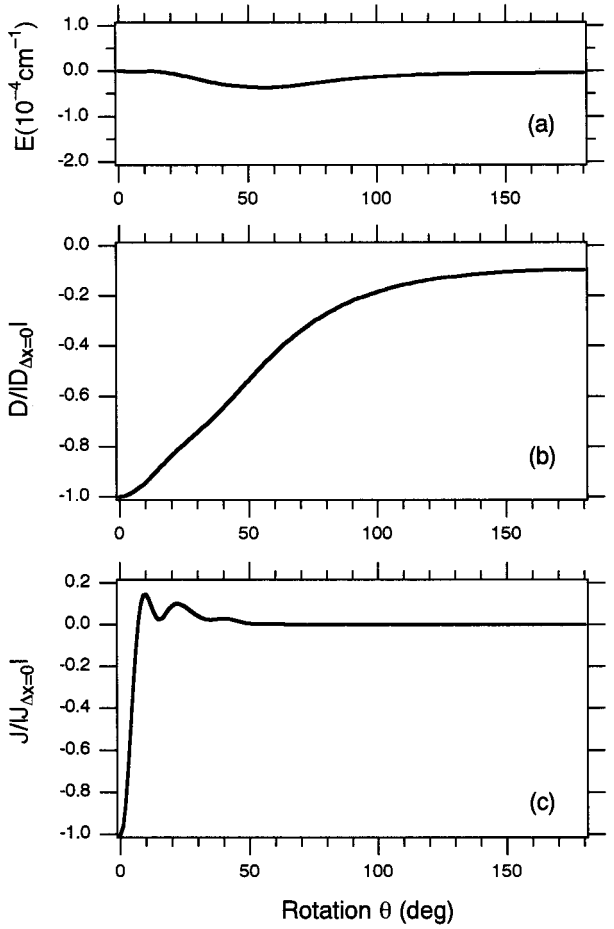

Figure 8. Plots of (a) zero-field splitting constant *E*, (b) *D* and (c) exchange interaction *J* in a function of rotation angle θ defined in Scheme 3. Δ*z* is set at 7.0 Å.

SCHEME 3

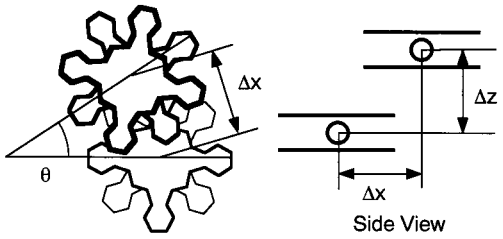

E, *D*, and *J* values with varied θ, which is defined in Scheme 3 and Figure 2 (bottom). The axis of rotation, which passes through both centers of the crown parts, is placed at 9.5 Å away from the center of the Pc part of each CR_1Pc ring. In all the region of θ, *E* takes a negative value, reaching maximum absolute value at $\theta = 60°$. The absolute value of *D* is decreasing with θ, and reaches 8% of $|D_{(\theta=0)}|$ at $\theta = 180°$. From the $|D|/|D_{(\theta=0)}|$ ratio of two cation-induced systems (0.00268/0.00407 = 0.66), θ is estimated at about 38°. The corresponding amount of slide in the *xy* plane is 5.8 Å (Δ*x* in Scheme 3): two $Lu(Pc)_2$ sites have an overlap which is the same degree as that in the solvent-induced aggregate of $Lu(CR_4Pc)(Pc)$. This indicate that the freedom of rotation around the pivot is actually restricted by the same potential which builds up the solvent-induced structure of $Lu(CR_4)(Pc)$.

The variation of the exchange interaction *J* with θ is shown in Figure 8c. A similar behavior to that of the solvent-induced aggregate of $Lu(CR_4Pc)(Pc)$ is seen. As the angle θ increases from zero, *J* rapidly reaches zero and then takes a positive value.

In the region $|\theta| > 7°$, J is positive and the system is in a triplet state. From the estimated value of θ, the ground state of the system is predicted to be triplet.

Conclusion

The tetra-crown Pc dimer generates two types of supramolecular structures depending of the condition. Both cases show ESR signals typical of the triplet electronic state, with different zero-field-splitting constants. The first one is the cation-induced aggregate, whose ESR signal is simulated with zfs constant $|D| = 0.00407$ cm^{-1} (in the K^+-induced case). The other type is the solvent-induced structure, which has a smaller zfs constant $|D| = 0.00288$ cm^{-1}. In each case, an anisotropy in the line width was observed. This suggests existence of an anisotropy in the hyper-fine interactions, which are incorporated in the Gaussian line-shape envelope in the actual simulation.

The mono-crown Pc dimer also gives a cation-induced structure with smaller zfs constant than that of the tetra-crown Pc dimer case. On the other hand, the solvent-induced aggregation was not as effective as in the tetra-crown case. This observation and the fact that unsubstituted $Lu(Pc)_2$ does not show such a phenomenon at all suggest that the number of crown parts is the determinative factor in the solvent-induced aggregate formation.

The geometric structures of the three types of aggregation above are investigated by the theoretical calculation. The hypothetical D_{4h} symmetry in the cation-induced system composed of $Lu(CR_4Pc)(Pc)$ was confirmed to be reasonable by the model calculation. The center-to-center distance in this case is estimated at 7.0 Å.

For the solvent-induced aggregate composed of $Lu(CR_4Pc)(Pc)$, a possibility of the structure where one $Lu(Pc)_2$ site is vertically above the counterpart site is excluded, since the calculation predicted unreasonably long distance with this hypothesis. A reasonable arrangement is the one where a $Lu(Pc)_2$ site slides horizontally keeping the interplanar distance. The calculations with this assumption predict that such slide is about 5 Å.

The K^+-induced structure composed of $Lu(CR_1Pc)(Pc)$ has a freedom of rotation around the pivot point on the potassium cation. The calculation showed the rotation angle θ is fixed at about 30°−40°. This indicates that angle $\theta = 180°$, which corresponds to the minimum steric hindrance, is not energetically favorable. It is suggested that the partial overlap between two $Lu(Pc)_2$ sites lowers the total energy of the system.

By the calculation of the exchange interaction J, we found that when an aggregate possesses a common C_4 axis, the ground state is singlet. By latitudinal displacement of the two $Lu(Pc)_2$ sites, the ground-state becomes triplet. The singlet and triplet states are switched also in the K^+-induced aggregation of $Lu(CR_1Pc)(Pc)$ by rotation around the pivot.

Acknowledgment. This work was partially supported by a Grant-in-Aid for Science Research No. 10740303 from the Ministry of Education, Science Sports and Culture in Japan.

Note Added After Web Posting. This article was inadvertently releseaed to the web on 10/07/00 with an incorrect version of Figure 3. The correct version of Figure 3 now appears. The correct version was post on 10/13/00.

References and Notes

(1) Chang, A. T.; Marchon, J.-C. *Inorg. Chim. Acta* **1981**, *53*, L241.
(2) Ishikawa, N.; Ohno, O.; Kaizu, Y. *Chem. Phys. Lett.* **1991**, *180*, 51.
(3) (a) André, J.-J.; Holczer, K.; Petit, P.; Riou, M.-T.; Clarisse, C.; Even, R.; Fourmigue, M.; Simon, J. *Chem. Phys. Lett.* **1985**, *115*, 463. (b) Turek, P.; Petit, P.; André, J.-J.; Simon, J.; Even, R.; Boudjema, B.; Guillaud, G.; Maitrot, M. *J. Am. Chem. Soc.* **1987**, *109*, 5119. (c) Maitrot, M.; Guillaud, G.; Boudjema, B.; André, J.-J.; Strzelecka, H.; Simon, J.; Even, R. *Chem. Phys. Lett.* **1987**, *133*, 59. (d) Petit, P.; Holczer, K.; André, J.-J. *J. Phys.* **1987**, *48*, 1363. (e) Petit, P.; Turek, Ph.; André, J.-J.; Even, R.; Simon, J.; Madru, R.; Al Sadoun, M.; Guillaud, G.; Maitrot, M. *Synth. Met.* **1989**, *29*, F59.
(4) Padilla, J.; Hatfield, W. E. *Synth. Met.* **1989**, *29*, F45.
(5) Robinet, S.; Clarisse, C. *Thin Solid Films* **1989**, *170*, L51.
(6) Paillaud, J. L.; Drillon, M.; De Cian, A.; Fischer, J.; Weiss, R.; Poinsot, R.; Herr, A. *Physica B* **1991**, *175*, 377.
(7) Ishikawa, N.; Kaizu, Y. *Chem. Lett*. **1998**, 183.
(8) Ishikawa, N.; Kaizu, Y. *Chem. Phys. Lett.* **1993**, *203*, 472.
(9) Kobayashi, N.; Lever, A. B. P. *J. Am. Chem. Soc.* **1987**, *109*, 7433.
(10) De Cian, A.; Moussavi, M.; Fischer, J.; Weiss, R. *Inorg. Chem.* **1985**, *24*, 3162.
(11) Ohno, O.; Ishikawa, N.; Matsuzawa, H.; Kaizu, Y.; Kobayashi, H. *J. Chem. Phys.* **1989**, *93*, 1713.
(12) Ishikawa, N.; Ohno, O.; Kaizu, Y.; Kobayashi, H. *J. Phys. Chem.* **1992**, *96*, 8832.
(13) Ishikawa, N.; Ohno, O.; Kaizu, Y. *J. Phys. Chem.* **1993**, *97*, 1004.
(14) Ishikawa, N.; Kaizu, Y. *Inorg. Chem.* **1999**, *38*, 3173.
(15) McWeeny, R. *Method of Molecular Quantum Mechanics*, 2nd ed.; Academic Press Inc.: London, 1992; Chapter 6.
(16) Used parameters are: for carbon atoms, ionization potential of z ($2p_z$) orbital $Ip = 11.22$ eV, one-center Coulomb integral $(zz|zz) = 10.60$ eV, and Slater's orbital exponent $\zeta = 1.625$; for nitrogen atoms, $Ip = 14.51$ eV, $(zz|zz) = 13.31$ eV, and $\zeta = 1.95$.
(17) Pilcher, C.; Skinner, H. A. *J. Inorg. Nucl. Chem.* **1962**, *24*, 937.
(18) According to Pilcher and Skinner,[17] the ionization potential of a process $(t_1^2t_2t_3z) \rightarrow (t_1^2t_2t_3)$ is 14.51 eV, that of $(t_1t_2t_3z^2) \rightarrow (t_1t_2t_3z)$ 12.25 eV, and the electron affinity of $(t_1^2t_2t_3z) \rightarrow (t_1^2t_2t_3z^2)$ 1.20 eV. Here t_1, t_2, and t_3 are sp^2 hybrid orbitals and z is a $2p_z$ orbital. These are expressed by an one-electron term Iz and two-electron terms $(tt|zz)$, $(tz|tz)$ and $(zz|zz)$ as follows: (i) $14.51 = -I_z - 4\{(tt|zz) - (tz|tz)/2\}$, (ii) $12.25 = -Iz - 3\{(tt|zz) - (tz|tz)/2\} - (zz|zz)$, and (iii) $1.20 = -Iz - 4\{(tt|zz) - (tz|tz)/2\} - (zz|zz)$. The effect of the donating charge q on the ionization potential (i) is expressed as $Ip = -Iz - (4 - q)\{(tt|zz) - (tz|tz)/2\} = 58.71 - 11.05(4 - q)$.
(19) Ishikawa, N.; Kaizu, Y. *J. Phys. Chem.* **1996**, *100*, 8722.
(20) Atherton, N. M. *Principles of Electron Spin Resonance*; Ellis Horwood PTR Prentice Hall: Englewood Cliffs, NJ, 1993; Section X.
(21) The definition of the "distance" here is the length of the perpendicular dropped from a lanthanide ion to the plane which contains the lanthanide ion of the adjacent complex and is perpendicular to the C_4 axes.
(22) De Cian, A.; Moussavi, M.; Fischer, J.; Weiss, R. *Inorg. Chem.* **1985**, *24*, 3162.
(23) Petit, P.; Holczer, K.; André, J.-J. *J. Physique* **1987**, *48*, 1363.
(24) Darovskikh, A. N.; Frank-Kamenetskaya, O.; V.; Fundamenskii, V. S. *Sov. Phys. Crystallogr.* **1986**, *31* (5), 534.
(25) Piechocki, C.; Simon, J.; André, J.-J.; Guillon, D.; Petit, P.; Skoulios, A.; Weber, P. *Chem. Phys. Lett.* **1985**, *122*, 124.
(26) Blake, A. J.; Gould, R. O.; Li, W.-S.; Lippolis, V.; Parsons, S.; Radek, C.; Schroder, M. *Angew. Chem., Int. Ed. Engl.* **1998**, *37*, 293.
(27) Mallinson, P. R.; Truter, M. R. *J. Chem. Soc., Perkin Trans.* 2 **1972**, 1818.
(28) Rogers, R. D.; Kurihara, L. K.; Benning, M. M. *Inorg. Chem.* **1987**, *26*, 4346.